

The mystery of the alkali metals; the induced anomalous Hall effect in thin Cs films

H. Beckmann^a and G. Bergmann

Department of Physics, University of Southern California, Los Angeles, California 90089-0484, USA

Received 29 April 1999 and Received in final form 10 July 1999

Abstract. Sandwiches made from Fe and Cs films are investigated as a function of the magnetic field and the Cs thickness. Conduction electrons which cross from the Fe to the Cs are marked by a drift velocity component perpendicular to the electric field. The anomalous Hall effect in the Fe provides this “non-diagonal” kick to the electrons that cross from the Fe into the Cs. The ballistic propagation of the conduction electrons can be monitored as a function of the Cs film thickness. The free propagation into the Cs is measured in terms of the non-diagonal conductance L_{xy} which we denote as the “induced anomalous Hall conductance” L_{xy}^0 . For a normal (non-magnetic) metal in contact with Fe, L_{xy} increases with the thickness of the normal metal until the film thickness exceeds (half) the mean free path of the conduction electrons. For Cs on top of Fe the induced anomalous Hall conductance increases up to a Cs coverage of about 100 Å, then, in contrast to other non-magnetic metals, L_{xy}^0 decreases for larger Cs coverage and approaches zero. This behavior cannot be explained with the free electron model. The strange behavior of the induced AHC in Cs films adds an even more challenging mystery to the already poorly understood properties of thin Cs films. These results defy explanation in the free electron model.

PACS. 71.20.Dg Alkali and alkaline earth metals – 72.10.Fk Scattering by point defects, dislocations, surfaces, and other imperfections (including Kondo effect) – 73.50.-h Electronic transport phenomena in thin films and low-dimensional structures

1 Introduction

The alkali metals are described in the majority of solid state text books as the best example of a nearly free electron system. DeHaas-van Alphen measurements [1, 2] yield Fermi surfaces for the alkali metals that deviate very little from a perfect sphere, for example for Na, by less 0.1%. Measurements of the transport properties yield, however, a mixed picture. While some can be described with the free electron model [3], others can not (see Overhauser’s review article [4]). Overhauser argues that the Coulomb interaction causes an instability in the electron system of the alkali metals which results in macroscopic charge-density waves, and he collected a large body of experimental data which support his model.

Our group recently observed some unusual properties in thin Cs films [5, 6]. Thin Cs films show a dramatic change in resistance and Hall effect when covered with 1/100 of a mono-layer of Ag, Au, In and Pb. Covering an 8.2 nm thick Cs film with 0.1 atomic layers of In increases the resistance by 58%, the Hall constant by 15%, the temperature dependence of the resistance by 12%, and the electron dephasing rate by 15%. The reason for this behavior is unknown. We considered the possibility that the surface atoms introduce diffuse surface scattering. A

detailed analysis showed, however, that this explanation requires too large a scattering cross section of the impurities and could not explain the increase of the Hall effect. Another hypothesis we tested was that the impurities passivate a finite thickness of the Cs at the surface. This yields the thickness of the passivated (insulating) layer to be about 3.0 nm for thin Cs films and about 6.0 nm for thicker ones. This explanation, however, requires that one impurity atom passivates about 30 Cs atoms, a rather unlikely scenario.

In the measurements of the resistance and the Hall constant one essentially investigates the propagation of the electrons parallel to the film. In contrast we perform in this paper a series of measurement in which we investigate the propagation of the conduction electrons perpendicular to the film plane. The method we use is the “induced anomalous Hall effect” [7]. To explain this method we will first recall the anomalous Hall effect in ferro-magnetic metals.

1.1 The anomalous Hall effect (AHE)

Figure 1 shows the Hall resistance R_{yx} as a function of the applied magnetic field B for a thin Fe film. The Fe film is quench condensed and has a thickness of 7.0 nm and a resistance of 108 Ω. One recognizes that the Hall resistance R_{yx} is positive, increases strongly at small fields,

^a e-mail: bergmann@usc.edu

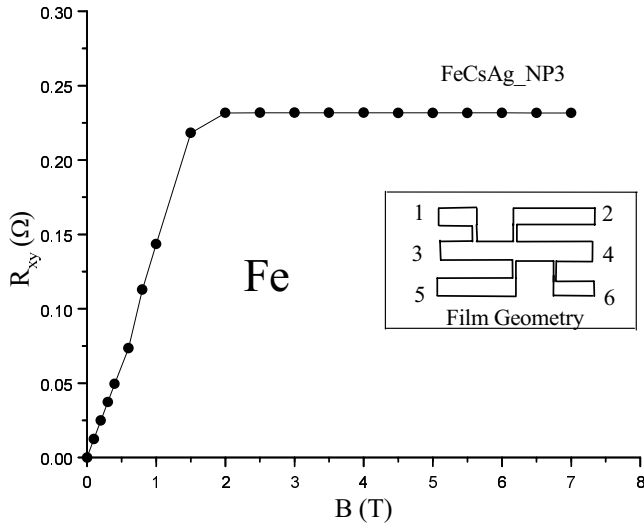


Fig. 1. The Hall curve of a quench condensed Fe film ($d_{\text{Fe}} = 7$ nm, $R_{xx} = 108$ Ω). The linear extrapolation from high magnetic fields B towards zero magnetic field yields the anomalous Hall resistance R_{yx}^0 in zero magnetic field. The insert shows the shape of the film with its electrodes. Electrodes (3, 4) are the current electrodes, the resistance can be measured with electrodes (1, 2) or (5, 6). A comparison checks the homogeneity of the film. The Hall resistance is measured with electrodes (2, 5).

and saturates at a field of about 2 T, the saturation magnetization J_0 of the Fe film. The Hall resistance consists of two contributions, (1) the anomalous Hall resistance which increases linearly between 0 and 2 T and saturates above 2 T and (2) the normal Hall resistance which remains linear throughout the whole field range.

The anomalous Hall resistance is caused by asymmetric scattering of the conduction electrons at the magnetic moments of the Fe atoms (for example see [8,9]). It is proportional to the z -component of the magnetization. For a thin film, which has a very high demagnetization factor, the z -component of the magnetization J is essentially equal to the magnetic flux B ($J_z = B$). This remains true as long as the magnetic flux is less than the saturation magnetization, *i.e.* for $B \leq J_0$. For $B > J_0$ the z -component of the magnetization takes the saturation value $J_z = J_0$. This explains the shape of the anomalous Hall resistance as a function of magnetic field in Figure 1. The saturation value of the anomalous Hall resistance in this Fe film is $R_{yx}^0 = 0.23$ Ω.

At fields above J_0 , one has two linear contributions to the Hall resistance: (a) the normal Hall resistance and (b) a high field contribution due to the anomalous Hall effect which is proportional to the high field susceptibility $\frac{dJ}{dB}$. Because we cannot separate the two we will denote the linear part of the Hall resistance as the “normal Hall resistance”. For the pure disordered Fe film in Figure 1, the slope of the normal Hall resistance is $\frac{dR_{yx}}{dB} = 0.0044 \frac{\Omega}{\text{T}}$. As such it is hidden in the figure.

One obtains the full anomalous Hall resistance only for fields larger than the saturation magnetization ($B > J_0$).

However, if one extrapolates the Hall curve from high fields back to the zero field then one obtains the anomalous Hall resistance R_{yx}^0 for the magnetization oriented perpendicular to the film at zero magnetic field. *This way one obtains the full anomalous Hall resistance in zero magnetic field* (a situation which can not be measured directly). When we refer in this paper to the anomalous Hall resistance (or conductance) in zero magnetic field, we are referring to this artificial (extrapolated) situation.

The saturation value of the Hall conductance L_{xy}^0 can be obtained from the ohmic resistance R_{xx} and the anomalous Hall resistance R_{yx}^0 :

$$L_{xy}^0 = \frac{R_{yx}^0}{(R_{xx})^2 + (R_{yx}^0)^2} \approx \frac{R_{yx}^0}{(R_{xx})^2}.$$

In the discussed Fe film this yields $L_{xy}^0 = 2.0 \times 10^{-5} \Omega^{-1}$.

If we define the x -direction as the direction of the electric field (and the z -direction as perpendicular to the film) the current I has not only an x -component I_x but also a y -component I_y , where $I_x = L_{xx}E$ and $I_y = L_{yx}E$. This is also true in zero magnetic field (and the saturation magnetization parallel to the z -direction).

1.2 Induced anomalous Hall effect

In the next step of our consideration we cover the Fe film with a normal film M. The resistances of the two films are in parallel. In the simplest description of this sandwich the conductance components L_{xx} and L_{xy} of the two films simply add up

$$L_{ij}(\text{sandwich}) = L_{ij}(\text{Fe}) + L_{ij}(\text{M}).$$

The normal film M has zero Hall conductance L_{xy} in zero magnetic field, so the total Hall conductance of the sandwich is just the Hall conductance of the Fe film. However, in reality the conduction electrons of the Fe and the M film cross the interface and transfer their momentum from one film to the other. In Figure 2 we have drawn the drift velocity \mathbf{v}_d of the conduction electrons of the Fe film in a cut through the Fermi surface of the s -electrons of the Fe at $k_z > 0$. Each electron has a component of \mathbf{v}_d in the x -direction and in the y -direction. (Generally, the two components depend on the spin of the conduction electron.) At the interface these conduction electrons enter the normal metal M. Here they propagate ballistically, maintaining their drift velocity until they are scattered (either by a defect or the free surface of M). As a consequence we find a y -component of the current in the normal metal, yielding a y -component of the conductance in the normal film. This is the induced anomalous Hall effect. One might say that we have marked the conduction electrons which pass from the Fe into the normal metal. When these marked electrons experience a (catastrophic or s -) scattering in the metal M their drift velocity is destroyed. By measuring the increase of the anomalous Hall conductance as a function of the normal film's thickness d_M , one

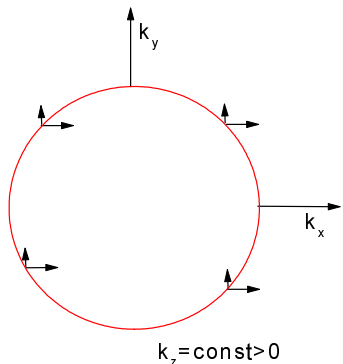


Fig. 2. The drift velocity of the conduction electron in the Fe film for $k_z > 0$ has not only a component in v_x in the direction of the electric field \mathbf{E} but also a Hall component v_y due to the anomalous Hall effect. If the electrons cross the interface to the normal metal they carry this y -component of the drift velocity into the normal metal and induce an anomalous Hall conductance.

may follow the propagation of the electrons from the interface into the normal metal. If we denote the mean free path in the normal metal with l_M then the induced Hall conductance saturates at a film thickness of about $l_M/2$.

2 Experiment

2.1 Film preparation and measurement

A typical experiment begins with the deposition of a thin Fe film onto a quartz substrate. The Fe is evaporated from a 1 mm Fe wire with a nominal purity of 99.99%. The substrate is a plate of crystalline quartz which is held at helium temperature. The Fe film has a thickness of about 9.0 nm. After the deposition it is annealed to 40 K. Its structure is fine crystalline. After annealing, the resistance per square is of the order of 100 Ω . The longitudinal and transverse (Hall) resistance of the Fe is then measured in the field range between $-7 \text{ T} < B < +7 \text{ T}$. A relatively large current is used to obtain a high sensitivity in the Hall resistance. For the temperatures of 4.5 K, 6.5 K and 9.5 K the film is solely heated by the measuring current. The maximum current density is about 400 A/mm² for the Fe film and reaches 1000 A/mm² for thick, low resistance FeCs sandwiches. At these high currents a good thermal equilibrium of film, quartz plate and thermometer is still maintained. For the temperatures above 9.5 K (14 K and 20 K) we keep the measuring current used at 9.5 K and apply in addition a heater at the back of the quartz plate. After the measurement the Fe film is covered in many step with the metal of investigation. In most cases we investigate the properties of Cs films with increasing thicknesses.

The Cs films are evaporated from SAES-Getters Cs evaporation sources. They are quench condensed onto a substrate at He temperature in an ultra high vacuum of better than 10^{-11} torr. After condensation the films are annealed for several minutes at 35 K.

2.2 Measurement of the Hall effect

The film or sandwich has a width of 2 mm and is connected with six electrodes (see insert in Fig. 1). The electrodes (2) and (5) are opposite to each other and are used for measuring the Hall voltage. The electrodes (5) and (6) have a separation of 5 mm and are used for measuring the resistance (per square after dividing by 2.5) and its dependence on the magnetic field. The electrodes (1) and (2) also have a separation of 5 mm. A comparison of the voltages (resistances) between (1, 2) and (5, 6) gives a check on the homogeneity of the film. A magnetic field is applied perpendicularly to the quartz plate (and the film). It is varied between $-7 \text{ T} < B < +7 \text{ T}$. For the Hall resistance we take the asymmetric part of the resistance between the electrodes (2) and (5), $R_{25}(B)$, *i.e.* $R_{yx}(B) = \frac{1}{2} [R_{25}(B) - R_{25}(-B)]$ where $R_{25}(B) = \frac{V_{25}}{I}$. For the longitudinal resistance we take the symmetric part of $R_{56}(B)$, *i.e.* $R_{xx}(B) = \frac{1}{2} [R_{56}(B) + R_{56}(-B)]$ where $R_{56}(B) = \frac{V_{56}}{2.5I}$. (V_{ij} are the measure voltages and I is the current). The Hall resistance and the ohmic resistance are measured for 39 different field values of B with a higher density of field points at smaller fields. *In the experiment we always measure the resistances R_{xx} and R_{yx} .* The corresponding conductances are then obtained by inversion of the resistance matrix.

2.3 The Induced AHE in non-magnetic metal films

Because some of our experimental results for the induced AHC in Cs are very unexpected and unusual, we will first present the proper behavior of the induced AHC in a normal film, such as Mg.

2.4 Induced AHE in Mg

In Figure 3 we have plotted the AHC of quench condensed Mg on top of a thin Fe film with the usual parameters. The error in the induced AHC is less than the size of the circles. As can be seen from the graph the AHC increases linearly with increasing Mg thickness and saturates for larger Mg thickness. (The saturation thickness is defined as the intercept of the initial slope at $d_{Mg} = 0$ and the final (horizontal) slope for large Mg thicknesses). This yields, in our example, the Mg saturation thickness of 4.2 nm. Another example is presented in reference [7] for a film of In on Fe.

2.5 Induced AHE in pure Cs

Now we investigate the induced AHC in Cs films on top of thin Fe films. Figure 4 shows the anomalous Hall curve for a sandwich consisting of FeCs, where an Fe film of 6.9 nm thickness has been covered with 18.1 nm of Cs. The resistance (per square) is 6.7 Ω . For this sandwich the linear slope of the original Hall curve (which is already subtracted) is $\frac{dR_{yx}}{dB} = -0.049 \frac{\Omega}{\text{T}}$ and the normal

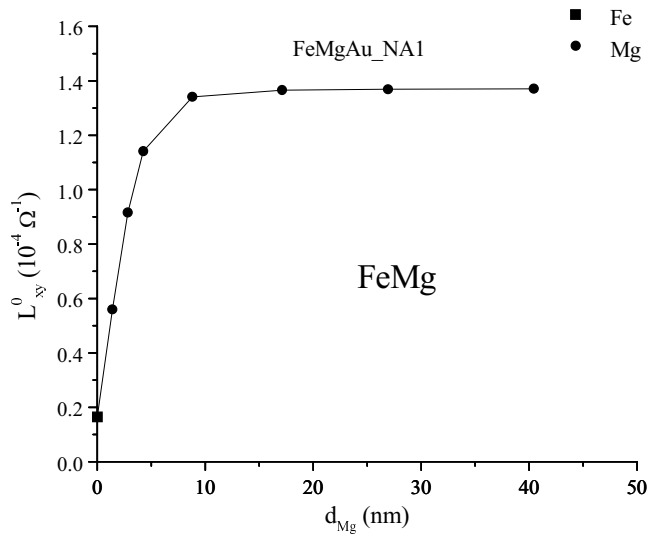


Fig. 3. The anomalous Hall conductance L_{xy}^0 of a FeMg sandwich as a function of the Mg thickness.

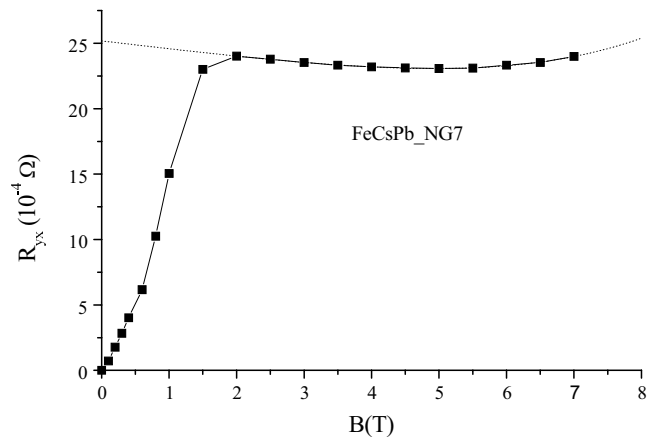


Fig. 4. The Hall resistance curve for a sandwich consisting of FeCs where the Fe film has been covered with 18.1 nm Cs. The resistance (per square) is 6.7 Ω .

Hall resistance at 7 T is $R_{yx}(7 \text{ T}) = -0.34 \Omega$. This value is much larger than the anomalous Hall resistance, whose extrapolated value is $R_{yx}^0 = 0.0025 \Omega$. In this sandwich the ratio of the anomalous Hall resistance to the normal Hall resistance at 7 T is only 0.0073. One recognizes that the high field part of the Hall resistance is curved. This is due to the slight non-linearity of the Hall resistance of pure Cs. Nevertheless the value of R_{yx}^0 can still be reliably extrapolated from the Hall curve (dashed curve). With increasing Cs thickness this non-linearity induces an uncertainty in the extrapolation. For FeCs sandwiches with a thickness of pure Cs in excess of 20.0 nm the extrapolation introduces an error which is shown in Figures 5 and 10 by error bars and which is discussed in the appendix.

Figure 5 presents a plot of the (extrapolated) AHC of pure Cs on top of Fe. This curve shows a behavior totally different than what we had naively expected.

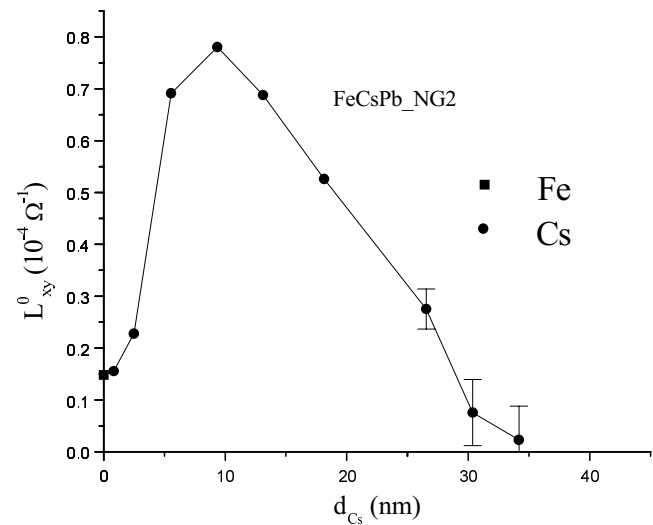


Fig. 5. The anomalous Hall conductance L_{xy}^0 of a FeCs sandwich as a function of the Cs thickness.

The AHC does not increase monotonically, approaching a saturation value. Instead, the AHC has a maximum at about 10 nm Cs thickness, and then decreases, approaching the x -axis above 30 nm Cs thickness. At $d_{Cs} = 34.0$ nm the resistance of the Cs film is 2.4 Ω and the error in the evaluation becomes too large (see error bars) to decide whether the AHC approaches the value 0, crosses into negative territory or increases again. The decrease of the AHC beyond the Cs thickness of 10 nm is, however, dramatic enough. This result has been reproduced in many different experiments.

2.6 Influence of the mean free path on the induced AHC in Cs

We next investigated experimentally whether we could influence this behavior by other experimental parameters. The first, and most obvious, parameter we tested was the mean free path l_{Cs} of the conduction electrons. We altered l_{Cs} in two different ways: (a) we evaporated alternating Cs and Na films and (b) we introduced Ag impurities into the Cs film.

2.6.1 FeCsNa sandwich

To reduce the transport mean free path in the alkali metal we condense alternating 4.0 nm films of Cs and 4.0 nm films of Na onto the Fe film. In this case the mean free path approaches 18.0 nm in the Cs film and 12.0 nm in the Na film (after the total coverage exceeds 10 nm). In Figure 6 the induced AHC is plotted as a function of the alkali coverage. The errors in the induced AHC are less than the size of the circles. The induced AHC shows the theoretical behavior, it saturates with increasing alkali thickness.

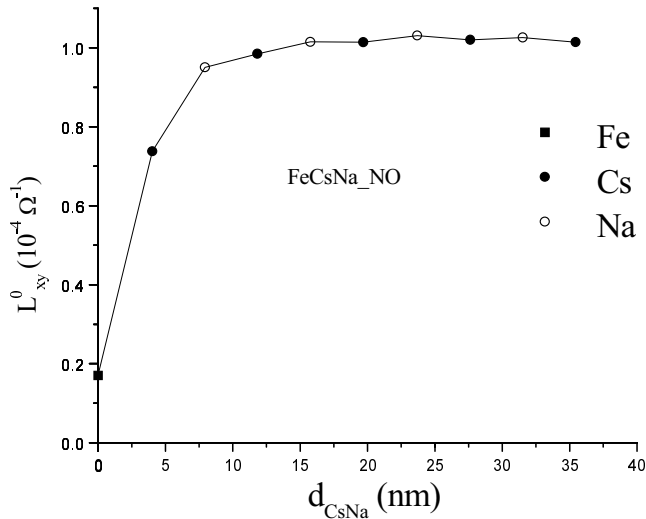


Fig. 6. The anomalous Hall conductance L_{xy}^0 of a FeCsNa sandwich as a function of the combined CsNa thickness.

2.6.2 FeCsAg sandwiches

In two sets of experiments we prepared $\text{Fe}(\text{CsAg})_n$ sandwiches. In the first one we alternated the evaporation of 5.0 nm Cs with 0.01 atomic layers of Ag. The result of the induced AHC is plotted in Figure 7. (For $n \leq 3$ the Hall curve was measured after each Cs and Ag evaporation. After this the Hall curve was only measured after the Cs evaporation.) One can easily recognize that the induced AHC qualitatively shows the same behavior as a coverage of pure Cs. A check of the transport mean free path shows that the l_{tr} is not dramatically reduced by the Ag impurities. At $d_{\text{Cs}} = 30$ nm, it has a value of $l_{\text{tr}} = 40$ nm. (l_{tr} increases almost linearly with the Cs thickness in this experiment). The error bars at the two largest Cs thickness is about the size of the circles.

We then repeated this experiment for a Ag coverage of 0.04 atomic layers. The resulting induced AHC is shown in Figure 8. One clearly sees that now the induced AHC almost saturates at Cs thickness $d_{\text{Cs}} > 10$ nm. The error bars lie within the circles. The transport mean free path of each individual Cs layer is shown in Figure 9. It approaches 30 nm after the Cs evaporation, reducing to about 20 nm after the Ag evaporation.

2.7 Indirect contact between Fe and Cs

In all the above experiments the Cs film was in direct contact with the Fe film. We cannot exclude that at the interface a direct exchange interaction between the Fe d -electrons and the Cs conduction electrons polarizes the latter. As a matter of fact, a simple Hartree-Fock calculation (without screening) [10] yields that a ferro-magnetic state of the conduction electrons has a lower energy in Cs than the non-magnetic state. Because of this, we performed two experiments in which the Fe and the Cs films were separated by an Ag or an Au film with a thickness

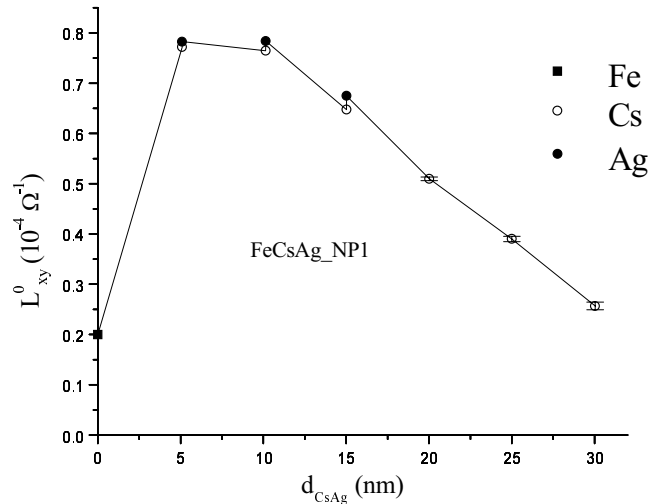


Fig. 7. The anomalous Hall conductance L_{xy}^0 of a $\text{Fe}(\text{CsAg})_n$ sandwich as a function of the CsAg thickness. The Cs and Ag evaporation alternate. The Cs is evaporated in steps of about 5.0 nm, the coverage per Ag evaporation is 0.01 atomic layers and the Ag atoms act as impurities.

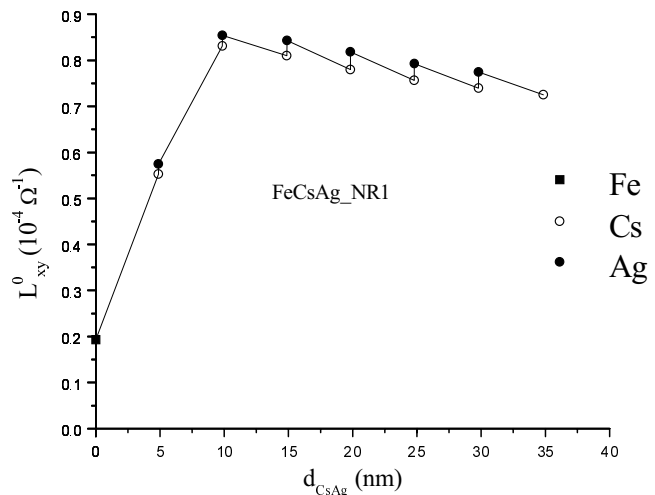


Fig. 8. The anomalous Hall conductance L_{xy}^0 of a $\text{Fe}(\text{CsAg})_n$ sandwich as a function of the CsAg thickness. The Cs and Ag evaporation alternate. The Cs is evaporated in steps of about 5.0 nm, the coverage per Ag evaporation is 0.04 atomic layers and the Ag atoms act as impurities.

of about 2 nm. Figure 10 shows the AHC for the FeAuCs system. One recognizes that, after a steep increase, the AHC shows a similar reduction as in the FeCs sandwiches without the Au layer. The error bars are similar as in the FeCs experiment in Figure 5.

3 Discussion

The decrease of the induced AHC in FeCs sandwiches for Cs thicknesses above 10 nm represents a very challenging puzzle, one which cannot be resolved within the free

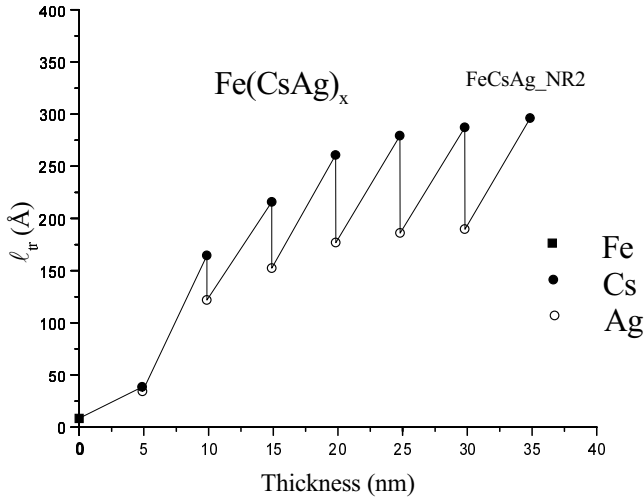


Fig. 9. The transport mean free path of $Fe(CsAg)_n$ sandwiches (from Fig. 8) as a function of the Cs coverage.

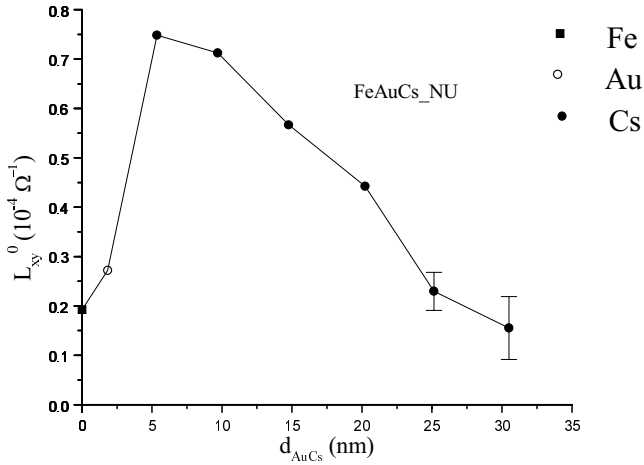


Fig. 10. The anomalous Hall conductance L_{xy}^0 of a FeAuCs sandwich as a function of the AuCs thickness.

electron model of Cs. To clarify this challenge we shall first summarize our main experimental results. Then we discuss different scenarios and attempts to explain the observed behavior. In the appendix we give a brief and simple theoretical description of the induced AHC.

3.1 Main results

The induced AHC for pure Cs on Fe does not show the ballistic behavior we expect. Our main experimental results are the following:

1. The induced AHC of FeCs sandwiches reaches a maximum at about 10 nm Cs thickness, then decreases for larger Cs thicknesses. For $d_{Cs} > 30$ nm, the induced AHC becomes undetectable (because of the increasing error for larger Cs thicknesses it cannot be determined whether L_{xy}^0 disappears).

2. For sandwiches consisting of FeCsNa, the induced AHC behaves as expected, *i.e.* it increases monotonically with CsNa thickness and saturates.
3. By introducing Ag impurities into FeCs sandwiches the mean free path of the Cs can be reduced to about 40 nm. This reduces the decrease in the induced AHC only slightly.
4. A reduction in the mean free path by Ag impurities in the Cs to about 25 nm removes most of the decrease in the induced AHC in FeCs sandwiches.
5. Separating the Fe and the Cs by introducing 2 nm of Au or Ag between them does not alter the decay of the induced AHC.

One of the authors [11] developed a simple model for the induced AHC. It is sketched in the appendix. There are many ways to improve this model. However, these improvements would only modify the quantitative results; they would not change the qualitative behavior. In contrast to the experiment, the induced AHC should always increase monotonically with the coverage of the (normal metal) Cs. An improvement of the theory within the free electron model of metal Cs can not remove this contradiction. Therefore we will not try to improve the model at the present time. Instead we need to find a new mechanism which explains the reversal of the induced AHC at Cs thicknesses above 10 nm.

3.2 Possible scenarios

We can imagine two different scenarios as being the origin of this perplexing behavior.

- 1. The Cs film is passive with respect to the anomalous Hall effect
- 2. The Cs film is actively contributing to the AHC.

In the first case, only the Fe film generates a drift velocity component in the y -direction. The contribution of the Cs is to manipulate this component in some unknown way. An example are

- Charge-density waves or spin-density waves.

In the second case the Cs actively generates a y -component to the drift velocity. Possible mechanisms are

- Induced spin current in Cs and spin-orbit-scattering
- Magnetic proximity effect.

3.3 Ideas that do not work

So far we have not succeeded in explaining the dependence of the induced AHC. We therefore had to consider a number of different models and ideas about Cs. In the following we shall give a short collection of our unsuccessful attempts.

3.3.1 Reflections by intersecting Bragg planes

Overhauser [12,13] predicted the existence of spin or charge density waves in the alkali metals. These new periodic structures generate a new pair of “Bragg planes” in the reciprocal lattice space which intersect the free electron sphere. The new Bragg planes are described by a wave vector \mathbf{Q} . Let us assume that it has a relatively small energy gap. An electron wave which emerges from the Fe film, and has the correct wave vector component $\mathbf{Q}/2$ parallel to \mathbf{Q} , will then be “reflected” with a small amplitude from each crest of the charge density wave. After a propagation time $\tau \approx \frac{\hbar}{\Delta\varepsilon}$, being inversely proportional to the energy gap, the whole electron wave is reflected. In a simple calculation we assumed that *every* electron, coming from the Fe film, reversed its component parallel to \mathbf{Q} . Even with this assumption we obtained a full cancellation of the induced AHC only when \mathbf{Q} was oriented parallel to \hat{y} . In a realistic calculation only a small fraction of the conduction electrons have the correct component of $\mathbf{Q}/2$ parallel to \mathbf{Q} , and one would obtain only a minor reduction of the induced AHC. Furthermore, Overhauser [13] suggests that in thin Cs films the \mathbf{Q} -vector is perpendicular to the film.

3.3.2 Magnetic proximity effect

Direct contact between the Fe and the Cs film could induce a magnetic state in the Cs close to the interface. Such a magnetic state causes an AHC in the Cs itself. If its sign is negative it could explain the reduction of the AHC with increasing Cs thickness. The fact that interlayers of 2 nm of Au and Ag between the Fe and the Cs hardly changed the induced AHC, however, makes this model unlikely.

3.3.3 Induced spin current in Cs and the spin-orbit-scattering

The Fe film has different potentials for spin up and down electrons. Thus, the spin of the induced Hall current I_y in the metal M (Cs) has a finite (expectation) value. If the electrons experience spin-orbit scattering in the Cs film then one can expect an asymmetric scattering in the Cs. The latter can yield an AHC.

The spin-orbit scattering can be directly measured in weak localization experiments. Recently, we performed a systematic investigation of weak localization in thin Cs films [6]. The result was that the spin-orbit scattering is too small to be detected in weak localization. This means that the spin-flip time is larger than 10^{-11} seconds. The time an electron needs to cross a Cs film of 20 nm thickness is about 10^{-14} s. So there are practically no spin-flip processes during the ballistic propagation of the electrons.

The crystalline Cs has a periodic spin-orbit potential and the electronic Bloch functions of the electrons in the Cs will be in a mixed spin state. This means that a spin up (down) electron which enters the Cs from the Fe will decompose into two different eigenstates of mixed spin

in the Cs with different kinetic energies and velocities (in analogy to different diffraction indices). We expect, however, that the phase difference that develops during a return trip from the Fe through the Cs film is too small to cause any effect.

4 Conclusion

In this paper we investigate the induced anomalous Hall effect in Cs films. The induced AHC for pure Cs on Fe does not show the ballistic behavior we expect. The induced AHC in FeCs sandwiches passes through a maximum at about 10 nm Cs thickness and decreases for larger Cs thickness. A reduction of the mean free path of the Cs in FeCs sandwiches to about 25 nm, for example by Ag impurities, removes most of the decrease in the induced AHC. These experimental results add to the mysterious properties of thin Cs films which are discussed in the introduction. The present investigation does not bring us closer to the solution of this puzzle but adds another dimension to the mystery. First investigations on Na films show similar results. Nevertheless these unexpected properties of Cs and other alkali films present a beautiful challenge. So far each new experiment raised more questions with no answers. Further experiments are needed to encircle the mystery of the alkali films.

The research was supported by NSF Grant No. DMR-9814260. We wish to express our appreciation to Dr. M. Huberman and Prof. A. Overhauser for many stimulating discussions.

Appendix A

A.1 The error in the induced AHC

For small Cs coverages (of the Fe film) the extrapolated AHC is very accurate and the error bar is smaller than the size of the circles in the figures. However, this changes for large coverages with pure Cs. The Hall curve of pure Cs films are not perfectly linear. The relative non-linearity (*i.e.* the ratio of the maximum deviation of the Hall resistance from the linear behavior divided by the Hall resistance at 7 T) is about $1-2 \times 10^{-3}$, even for Cs films with very short mean free paths (another unusual behavior of Cs films which is not yet understood). This introduces an uncertainty in the linear extrapolation of the anomalous Hall resistance.

For a Cs film of 30 nm thickness we find a normal Hall conductance of about $0.025 \Omega^{-1}$ at 7 T. The AHC

of the pure Fe film is about $1.5 \times 10^{-5} \Omega^{-1}$. The ratio is 0.0006. The AHC (of the Fe) is a factor 2-3 smaller than the non-linearity of the normal Hall conductance. This introduces an error in the extrapolation which is shown in Figures 5 and 10 by the error bars. If no error bar is shown then the error is smaller than the size of the circles. For pure Cs films (on top of Fe) with a thickness above 30 nm the extrapolation becomes unreliable. The error becomes larger than the actual value of the AHC.

A.2 Theory review of the induced AHC

One of the authors [7] developed a rather simple model for the induced AHC. The following assumptions are used in the model:

- A ferromagnetic metal F is covered with a non-magnetic metal M of thickness d_M ;
- the electron density (and consequently the Fermi surface) of ferromagnet F and normal metal M are set equal;
- the conduction electrons can propagate through the interface between the two metals without reflection;
- at the interface a fraction r of the conduction electrons can be scattered;
- the conduction electrons propagate ballistically until they are scattered by defects or reach the free surface of the metal M;
- the “free” surfaces of the ferro-magnet and of the normal metal scatter the conduction electron diffusively;
- the anomalous Hall effect in the ferro-magnet F is simulated by a (large) local magnetic field in F perpendicular to the interface (parallel to the magnetization) which yields a Hall angle ϕ_F in the ferro-magnet. Otherwise the conduction electrons in the Fe are treated as free electrons;
- the ferro-magnet and the normal metal have the mean free paths l_F and l_M ;
- all scattering processes are assumed to catastrophically (s -scattering);
- the vector-mean-free path method is used to calculate the total conductance tensor (\mathbf{L}) for the sandwich.

The conclusions of this model are that the anomalous Hall conductance of the sandwich increases due to the normal metal M.

$$\Delta L_{xy} = \frac{1}{2} r (A_F + A_M) l_F l_M \phi_F T \left(\frac{d_M}{l_M} \right)$$

$$T(s) = \frac{3}{2} \int_0^1 du (1-u^2) u (1 - e^{-s/u})$$

$$T(\infty) = \frac{3}{8}, \quad \frac{dT(s)}{ds} = 1$$

$$A_{F,M} = \frac{e^2 k_{F,M}^2}{3\pi^2 \hbar} = \frac{e^2}{12\pi^3 \hbar} S_{F,M}$$

Here ϕ_F is the anomalous Hall angle in the ferro-magnet. (No distinction is made between spin up and spin down electrons.) The prefactors A_F and A_M are essentially the area of the Fermi surface of F and M. The function $T(s)$ was essentially introduced by Fuchs [14] when he calculated the resistance of a thin film with partially diffusive scattering at the surface.

The following abbreviations are used: AHE = anomalous Hall effect; AHC = anomalous Hall conductance.

References

1. M.J.G. Lee, Proc. R. Soc. **A295**, 440 (1966).
2. A.P. Cracknell, Adv. Phys. **18**, 681 (1969).
3. J. Bass, W.P. Pratt, A.P. Schroeder, Rev. Mod. Phys. **62**, 645 (1990).
4. A.W. Overhauser, Adv. Phys. **27**, 343 (1978).
5. G. Bergmann, D. Frank, D. Garrett, Eur. Phys. J. B **3**, 345 (1998).
6. H. Beckmann, T. Fulmer, D. Garrett, M. Hossain, G. Bergmann, Phys. Rev. B **59**, 7724 (1999).
7. G. Bergmann, Phys. Rev. Lett. **41**, 1619 (1978).
8. J. Smit, Physica **16**, 612 (1951).
9. G. Bergmann, Phys. Today **32**, 25 (1979).
10. N.W. Ashcroft, N.D. Mermin, *Solid State Physics* (Saunders College, Philadelphia), Chapter 32, p. 682 (1976).
11. G. Bergmann, Phys. Rev. B **19**, 3933 (1979).
12. A.W. Overhauser, Phys. Rev. Lett. **4**, 462 (1960).
13. A.W. Overhauser, Phys. Rev. **128**, 1437 (1962).
14. K. Fuchs, Proc. Cambridge Phil. Soc. **34**, 100 (1938).